32ND INTERNATIONAL COSMIC RAY CONFERENCE, BEIJING 2011

The Shadow of the Moon in Cosmic Rays measured with IceCube

THE ICECUBE COLLABORATION[1], H. STIEBEL[2]
[1]*See special section in these proceedings*
[2]*Stockholm University, Department of Physics, SE 106 91 Stockholm, Sweden*

Abstract: The observation of a deficit of cosmic rays from the direction of the Moon is an important experimental verification of the absolute pointing accuracy of the IceCube detector and the angular resolution of the reconstruction methods. This Moon shadow in the downward-going muon flux has been observed with a statistical significance of more than 10 sigma in an initial analysis based on a binned counting approach. An unbinned maximum likelihood method was developed to reconstruct the shape and the position of this shadow more precisely, to compare the performance of different reconstruction algorithms and to verify the correctness of the angular error estimate.

Corresponding Authors: D.J. Boersma[3] (*boersma@icecube.wisc.edu*), L.E. Gladstone[4] (*gladstone@icecube.wisc.edu*), J. Blumenthal[3] (*blumenthal@physik.rwth-aachen.de*), H. Stiebel[2] (*hust7801@student.su.se*)
[3]RWTH Aachen University, III. Phys. Institut B, Otto-Blumenthal-Strae, 52074 Aachen, Germany
[4]UW Madison, 222 West Washington Avenue, Madison 53703 WI, USA
DOI: 10.7529/ICRC2011/V04/1235

Keywords: IceCube, cosmic rays, Moon shadow, pointing capability, neutrino astronomy

1 Introduction

IceCube [1] is a cubic kilometer scale Cherenkov detector at the geographical South Pole, designed to search for muons from high energy neutrino interactions. The arrival directions of these muons, which are reconstructed with $\mathcal{O}(1^\circ)$ accuracy, are used to search for point sources of astrophysical neutrinos [2], one of the primary goals of IceCube.

The main component of IceCube is an array of 5160 Digital Optical Modules (DOMs) deployed in the glacial ice at depths between 1450 m and 2450 m. During construction, with the first string of 60 DOMs deployed in January 2005 and the 86th and final string deployed in December 2010, the detector already took high quality data. The data analyzed and reported here were taken in the 40 and 59 string configurations, which were in operation between April 2008 and June 2010, with a configuration switch in May 2009.

For downward-going directions, the vast majority of the detected muons do not originate from neutrino interactions, but from high energy cosmic ray interactions in the atmosphere. While these cosmic ray muons are the dominant background in the search for astrophysical neutrinos, they can be used to study the performance of our detector. In particular, we can verify the pointing capability of IceCube by studying the shadow of the Moon in cosmic ray muons.

Cosmic rays at TeV energies propagate through the solar system nearly uniformly in all directions. The Moon blocks some cosmic rays from reaching the Earth. This creates the shadow of the Moon, a relative deficit of cosmic ray muons from the direction of the Moon.

The idea of a Moon shadow was first proposed in 1957 [3], and has become an established observation for a number of astroparticle physics experiments [4, 5, 6, 7]. Experiments have used the Moon shadow to calibrate detector angular resolution and pointing accuracy [8]. The shift of the Moon shadow due to the Earth magnetic field has also been observed [9].

For an observer at the geographic South Pole, the Moon rises and sets once per orbital period of 27.32 days. The number of cosmic ray induced muons reaching IceCube decreases with increasing declination (i.e. for increasingly horizontal directions), since the Earth and the Antarctic ice sheet filter low energy muons. Therefore, the shadow of the Moon is best observed as far above the horizon as possible, i.e. at low declinations. However, the minimum declination of the Moon in an orbital period varies slowly over time with a period of 18.6 years and is currently increasing. In April 2008, 2009 and 2010 the minimum declination of the Moon was -26.89°, -25.85° and -24.47°, respectively. Fig. 1 shows the energy spectrum of cosmic ray primaries that result in one or more muons triggering IceCube. For the declination greater than -30°, the energy threshold is about 2 TeV.

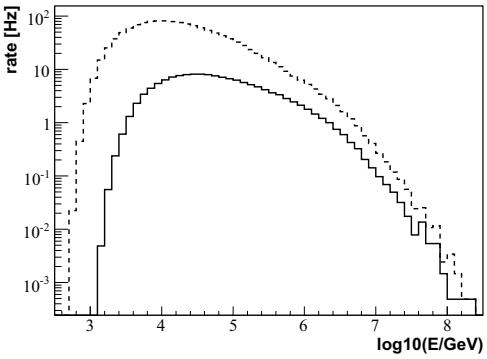

Figure 1: The energy spectrum of cosmic ray (CR) primaries with muons triggering IceCube, as simulated using CORSIKA [10]. Dashed: all events; solid: primaries with $\delta_{\rm CR} > -30^\circ$.

The Moon shadow in cosmic rays was first observed with IceCube using data taken during the first 8 orbital periods in the 40-string configuration, using a binned analysis [11]. In the analysis using the full data sets from the 40-string and 59-string configurations, a log-likelihood based analysis [12] has now been developed to study the point spread function of IceCube for muons.

The observed Moon shadow can be characterized with the following observables:

- The apparent shift of the Moon shadow from its nominal position (as computed from the time at which each muon event was recorded). A shift of order 0.1° is expected due to the Earth's magnetic field. Other contributions to a shift could come from e.g. a possible bias in track reconstruction or an error in the clock used to record the event times.
- The apparent width and ellipticity of the shadow. The apparent radius of the Moon is $\sim 0.25^\circ$, significantly smaller than the estimated angular resolution for muon tracks in IceCube. Hence the width of the shadow provides an experimentalal verification of the angular resolution estimate, which could for instance be different in zenith and azimuth directions.
- The number of shadowed events should be compatible with the measured flux of cosmic-ray induced muons (at the declination of the Moon) and the solid angle subtended by the Moon. Any significantly deviating result would be an indication of a systematic error.

2 Event selection

The trigger rate from cosmic ray muons was about 1.2-1.3 kHz in the 40-string configuration and close to 2 kHz in the 59 string configuration. However, most of those muons detected by IceCube travel nearly vertically, and thus they cannot have come from directions near the Moon.

The online event selection is defined as follows:

- the Moon must be at least 15° above the horizon
- at least 12 DOMs must register each event
- at least 3 strings must contain hit DOMs
- the reconstructed direction must be within 10° of the Moon in declination
- the reconstructed direction must be within $40^\circ / \cos(\delta_\mu)$ of the Moon in right ascension; the $\cos(\delta_\mu)$ factor corrects for spherical projection effects

where δ_μ denotes the declination of the reconstructed track.

The online Moon shadow filter was active (i.e., the Moon was more than 15° above the horizon) for 7-9 days during each 27.3 day orbital period. In that time, between 10M and 20M events were selected, depending on the number of active installed strings, atmospheric conditions and detector stability. This is about one percent of all events triggering IceCube during those days.

The event sample that passed online selection is subject to the same higher level track fitting algorithms as used in the searches for point sources of astrophysical neutrinos. The track likelihood function used in the fit is based on a simplified model of the scattering and absorption of light in ice [13]. In the offline processing, the track fit is repeated using several different seeds. For the majority of the events, this leads to a solution which is close to the online fit with a slightly improved angular resolution, when studied in simulated data. For a fraction of all events, the track fit is ambiguous and the iterative fit may yield a completely different direction.

In the Moon shadow analysis, we characterize each event by the zenith angle difference $\Delta\theta = \theta_{\leftmoon} - \theta_\mu$ (which is equivalent to the the declination difference, thanks to the unique geographic location of the detector) and the azimuth angle difference $\Delta\phi = (\phi_{\leftmoon} - \phi_\mu) \cdot \sin\theta_\mu$ between the direction of the offline reconstructed track and the nominal position of the Moon at the time of the event.

In the analysis, on-source and off-source subsamples are defined using the offline reconstruction. They are again defined by an angular window, namely $|\Delta\theta| \leq 8^\circ$ and $|\Delta\phi + \phi_{\rm off}| \leq 8^\circ$. Here $\phi_{\rm off} = 0^\circ$ for the on-source sample, and $\phi_{\rm off} = \pm 18^\circ$ for the left and right half of the off-source sample, respectively. The on-source samples for the full year data sets of the 40-strings and 59 strings configurations contain 19M and 22M events, respectively.

The per-event directional error estimate is derived from the variation of the track likelihood function near the solution obtained with the track fit [14]. It can be characterized either by the 3 parameters describing the 1σ error ellipse, or by a single average angular error estimate. In this work, we use the latter characterization.

The reliability of the directional error estimate was studied in simulated data, and simple quality selection criteria were developed to ensure that the pull (ratio of real and estimated angular error) is on average equal to unity. Moreover, for numerical stability, only events with an error estimate in the range from 0.075° to 1.5° were accepted. About half of the events in the on-source and off-source samples satisfy all these criteria.

3 Likelihood analysis

An unbinned likelihood analysis was applied to both data sets, using an approach similar to the likelihood approach taken for the IceCube point source searches [2]. The likelihood for the Moon having shadowed n_s events centered around $\vec{x}_s$ out of the on-source data sample is expressed as:

$$L(\vec{x}_s, n_s) = \sum_i^N \log\left(\frac{n_s}{N} S_i + (1 - \frac{n_s}{N}) B_i\right), \quad (1)$$

where $\vec{x}_s = (\Delta\theta, \Delta\phi)$ is the position relative to the nominal Moon position, n_s is the number of signal events, N is the total number of events, S_i is the signal probability density, and B_i is the background probability density. Note that Eq. 1 includes no explicit energy-dependent term; this a major difference between the IceCube Moon analysis and the IceCube point source searches. For the Moon shadow, we expect the number of signal events to be negative, as the Moon produces a deficit.

The signal probability density function S_i was assumed to be Gaussian, with a width given for each event by the estimated error on the reconstructed position [14]. The background probability density function B_i was estimated by using the normalized (Moon-centered) declination distribution obtained from the two off-source regions, and by assuming a uniform distribution in (Moon-centered) right ascension.

The likelihood (1) was maximized at every point $\vec{x}_s$ in an angular grid around the nominal Moon position, allowing the number of "signal" events n_s to vary.

4 Results

The distribution of the reconstructed number of signal events n_s is shown in Figures 2 and 3 as a function of the offset coordinates of the center of the shadow from the nominal Moon position. The shadow of the Moon is observed as a significant deficit centered at the nominal Moon position.

These results are directly compared with the same distributions from the off-source samples, as shown in Fig. 4. The distributions of the off-source samples are consistent with null shadowing effect from the Moon. The RMS values of the n_s distributions obtained for the left and right halves the off-source are considered as two independent estimates of the standard deviation of the background fluctuations.

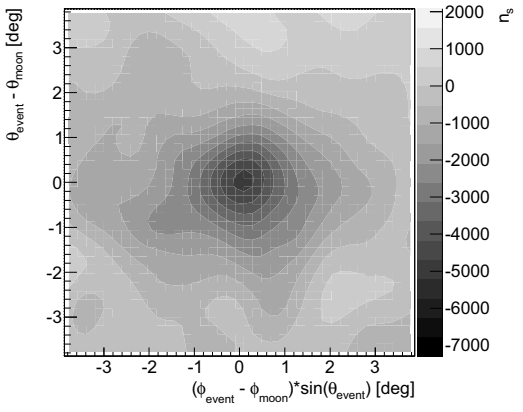

Figure 2: The Moon Shadow from the 40-string configuration *(preliminary)*. See text for details.

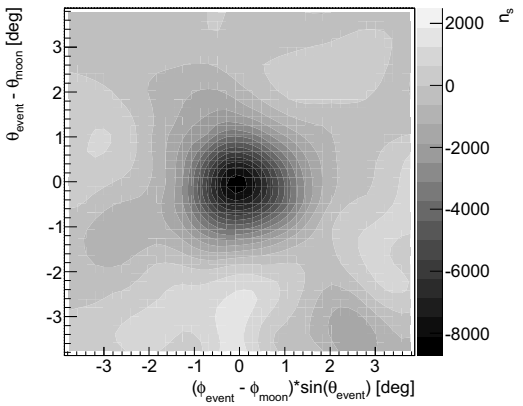

Figure 3: The Moon Shadow from the 59-string configuration *(preliminary)*. See text for details.

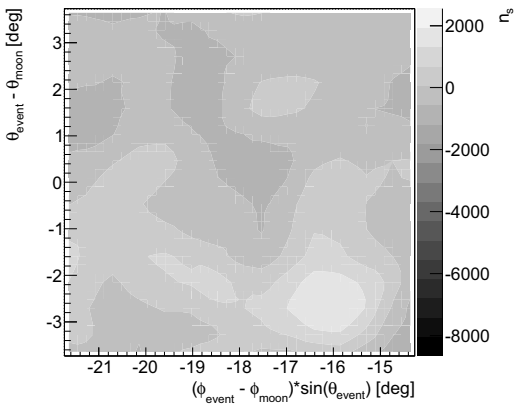

Figure 4: Fluctuation in n_s around the background model in one half of the off-source sample for the 59-string data set *(preliminary)*. See text for details.

	40 strings	59 strings
orbital periods	15	14
expected deficit	5734 ± 76	8192 ± 91
observed deficit	$5326 \pm 544 \pm 498$	$8660 \pm 565 \pm 681$
significance	10-11σ	13-15σ
θ offset	0.0°	0.0°
ϕ offset	0.0°	0.0°

Table 1: Results obtained in the Moon shadow analyses of the 40-string and 59-string data sets. Note that the two uncertainties given for the observed deficit are the estimates for the statistical uncertainty obtained from the left and right half of the off-source data samples; the numbers do *not* specify a systematic error.

The distributions of these values have means compatible with zero, as expected for the off-source regions. The RMS values of these distributions are now used as two independent estimates of the standard deviation of the background fluctuations (see Table 1).

The number of shadowed events found through likelihood maximization are also compared with the *expected* number of shadowed events. The expected number is calculated from the average apparent radius of the Moon and the off-source flux of downward-going muons from the declination of the Moon.

The depth of the observed shadow is compatible with the expected number of shadowed events. The significances of the shadows shown in Figures 2 and 3 are calculated to be 10-11σ and 13-15σ, respectively. The results for both detector configurations are summarized in Table 1.

The larger number of strings is the main reason for the larger significance of the result with the 59-strings configuration. With more optical sensors, more events are recorded, which are reconstructed with better angular resolution. On the other hand, the minimum declination reached by the Moon between April 2008 and May 2009 was more than a degree less than between May 2009 and June 2010. Moreover, the 40-string data sample contains livetime from one more orbital period.

To further confirm our results, the data from the 40-string configuration have also been analyzed using a different track fit algorithm and a corresponding angular error estimate. Simulation studies of this different reconstruction algorithm indicated an average pull of 1.55. Without correcting for this pull, the Moon shadow analysis resulted in a central n_s value of -3574 ± 434, differing by more than 5 standard deviations from the expectation: -6373 ± 80. Redoing the analysis with the angular error estimates rescaled by a factor of 1.55 resulted in a fitted n_s value compatible with expectation.

The log-likelihood-based analysis relies on the error estimate of the reconstructed track direction, ranging in this data sample from 0.075° to 1.5°. If we were not correctly estimating the angular errors, then we would find a shadow depth which is significantly smaller than expectation. The agreement between expected and observed shadow depth is a verification of the directional error estimate of the default track reconstruction algorithm as used in the analyses of the data taken with IceCube in these configurations.

5 Conclusions and Outlook

The shadow of the Moon in cosmic rays has been observed with a significance of more than 10σ in IceCube data collected between April 2008 and June 2010. The shadow depth is compatible with the expected number of shadowed events and has no significant systematic offset. These results confirm the pointing capability of IceCube.

We have started performing an observation of the shadow of the Sun. The shadow depth of the Sun should be comparable to that of the Moon, but a larger offset is expected due to the solar magnetic field. This offset should be correlated to the energy of the observed muons. Furthermore, if there is a component of high energy antiprotons in cosmic rays, then this should result in a faint second shadow with the opposite offset.

References

[1] H. Kolanoski, IceCube summary talk, these proceedings.

[2] J. Braun *et al.*, Astroparticle Physics **29** (2008) 299-305, [arXiv:0801.1604 [astro-ph]].

[3] G.W. Clark, Physical Review **108** (1957) p. 450-457.

[4] A. Karle for the HEGRA collaboration, Ann Arbor Proceedings (1990), High Energy Gamma-Ray Astronomy, p. 127-131.

[5] N. Giglietto, Nuclear Physics B Proceedings Supplements, Volume **61** (1997), Issue 3, p. 180-184.

[6] M.O. Wasco for the Milagro collaboration, 1999, arXiv:astro-ph/9906.388v1.

[7] The Soudan 2 collaboration, 1999, arXiv:hep-ex/9905.044v1.

[8] The Tibet AS Gamma Collaboration, M. Amenomori *et al.*, arXiv:astro-ph/0810.3757v1.

[9] L3 Collaboration, P. Achard *et al.*, Astropart. Phys. **23** (2005) p. 411-434, arXiv:astro-ph/0503472v1.

[10] D. Heck, J. Knapp, J.N. Capdevielle, G. Schatz, T. Thouw, FZKA **6019** (1998).

[11] D.J. Boersma, L. Gladstone, A. Karle, for the IceCube Collaboration, Proceedings of the 31^{st} ICRC, LODZ, POLAND (2009), arXiv:1002.4900.

[12] J. Blumenthal, Diplomarbeit in Physik (2011), Rheinisch-Westfälischen Technischen Hochschule Aachen, available upon request.

[13] G. Japaridze, M. Ribordy, arXiv:astro-ph/0506136v1.

[14] T. Neunhöffer and L. Köpke, Nuclear Instruments and Methods **A558** (2006) p. 561-568.

[15] H. Stiebel, Master Thesis (2011), Stockholm University, available upon request.